Session 3A: STARS
Convection

Comm. in Asteroseismology
Vol. 157, 2008, Wrocław HELAS Workshop 2008
M. Breger, W. Dziembowski, & M. Thompson, eds.

Modeling stochastic excitation of acoustic modes in stars: present status and perspectives

R. Samadi[1], K. Belkacem[1], M.-J. Goupil[1], H.-G. Ludwig[2] , and M.-A. Dupret[1]

[1] Observatoire de Paris, LESIA, CNRS UMR 8109, 92195 Meudon, France
[2] Observatoire de Paris, GEPI, CNRS UMR 8111, 92195 Meudon, France

Abstract

Solar-like oscillations have now been detected for more than ten years and their frequencies measured for a still growing number of stars with various characteristics (e.g. mass, chemical composition, evolutionary stage ...). Excitation of such oscillations is attributed to turbulent convection and takes place in the uppermost part of the convective envelope. Since the pioneering work of Goldreich & Keely (1977), more sophisticated theoretical models of stochastic excitation were developed, which differ from each other both by the way turbulent convection is modeled and by the assumed sources of excitation. We briefly review here the different underlying approximations and assumptions of those models. A second part shows that computed mode excitation rates crucially depend on the way time-correlations between eddies are described but also on the surface metal abundance of the star.

Individual Objects: Sun, α Cen A, HD 49933

Introduction

Solar p-modes are known to have finite lifetimes (a few days) and a very low amplitude (a few cm/s in velocity and a few ppm in brightness). In the last decade, solar-like oscillations have been detected in numerous stars, in different evolutionary stages and with different metallicity (see recent review by Bedding & Kjeldsen, 2007). Their finite lifetimes are a consequence of several complex damping processes that are not clearly identified so far. Their excitation is attributed to turbulent convection and takes place in the uppermost part of the convective envelope, which is the place of vigorous turbulent motions.

Measuring the mode amplitude and the mode lifetime enables to infer the excitation rate, $\mathcal{P}$ (the energy which is supplied per unit time to the mode). Deriving $\mathcal{P}$ put constraints on the theoretical models of mode excitation by turbulent convection (Libbrecht, 1988).

Goldreich & Keeley (1977, GK hereafter) have proposed the first theoretical model of stochastic excitation of solar acoustic modes by the Reynolds stresses. Since this pioneering work, different improved models have been proposed (Dolginov & Muslimov, 1984; Balmforth, 1992; Goldreich et al., 1994; Samadi & Goupil, 2001; Chaplin et al., 2005; Samadi et al., 2003; Belkacem et al., 2006b, 2008). These approaches differ from each other either by the way turbulent convection is described, or by the excitation process. In the present paper, we briefly review the main assumptions and approximations on which the different theoretical models are based.

As shown by Samadi et al. (2003), the energy supplied per time unit to the modes by turbulent convection crucially depends on the way eddies are time-correlated. A realistic

modeling of the eddy time-correlation at various length scales is then an important issue, which is discussed in details below. The structure and the properties of the convective upper envelope also has an important impact on the mode driving. In particular, the surface metal abundance can significantly change the efficiency of the mode driving.

Theoretical models

Most of the theoretical models of stochastic excitation adopt GK's approach. This approach first consists in solving, with appropriate boundary conditions, the equation that governs the *adiabatic* wave propagation (also called the homogeneous wave equation). This provides the well-known adiabatic displacement eigenvectors ($\vec{\xi}(\vec{r},t)$). Then, one includes in the wave equation turbulent sources of driving as well as a term of linear damping. The complete equation (so-called inhomogeneous wave equation) is then solved.

Among the sources of driving, the contribution of Reynolds stresses, which represents a mechanical source of driving, is considered. Goldreich et al. (1994, GMK hereafter) have proposed to include in addition the entropy fluctuations (also referred to as non-adiabatic gas pressure fluctuations). It is generally assumed that the entropy fluctuations behave as a passive scalar. In that case, Samadi & Goupil (2001, SG hereafter) have shown that the contribution of the *Lagrangian* entropy fluctuations vanishes. On the other hand, as shown by SG, the advection of the entropy fluctuations by the turbulent velocity field contributes efficiently to the mode driving in addition to the Reynolds stresses. This advective term corresponds to the buoyancy force associated with the entropy fluctuations. Since it involves the entropy fluctuations, it can be considered as a thermal source of driving.

The solution of the inhomogeneous wave equation corresponds to the forced mode displacement, $\delta\vec{r}$ (or equivalently the mode velocity $\vec{v}_{\rm osc} = d\delta\vec{r}/dt$). A detailed derivation of the solution for *radial* acoustic modes can be found in Samadi & Goupil (2001, SG herefater) or in Chaplin et al. (2005, CHE hereafter). It can be written as

$$\left\langle || \vec{v}_{\rm osc} ||^2 \right\rangle (\omega_0) \quad = \quad || \vec{\xi} ||^2 \ \frac{\mathcal{P}}{2\,\eta\, I} = \frac{|| \vec{\xi} ||^2}{16\,\eta\, I^2}\,(C_R^2 + C_S^2)\,, \tag{1}$$

where ω_0 is the mode frequency, $\mathcal{P}$ is the mode excitation rate (the rate at which energy is supplied to the mode), η the mode damping rate (which can be derived from seismic data), I the mode inertia, and finally C_R^2 and C_S^2 the contribution of the Reynolds stress and the entropy fluctuations, respectively. The expressions for C_R^2 and C_S^2 are

$$C_R^2 \quad = \quad 4\,\pi^3\,\mathcal{G} \int_0^M dm\,\rho_0 \left(\frac{d\xi_r}{dr}\right)^2 S_R(r,\omega_0) \tag{2}$$

$$C_S^2 \quad = \quad \frac{4\,\pi^3\,\mathcal{H}}{\omega_0^2} \int_0^M dm\,\frac{\alpha_s^2}{\rho_0}\, g_r\, S_S(r,\omega_0) \tag{3}$$

where $\alpha_s = (\partial P_g/\partial s)_\rho$, P_g is the gas pressure, s the entropy, ρ_0 the mean density, $\mathcal{G}$ and $\mathcal{H}$ are two anisotropic factors (see their expression in SG), S_R and S_S are the "source terms" associated with the Reynolds stresses and entropy fluctuations respectively, ξ_r the adiabatic mode radial eigen-displacement, and finally $g_r(\xi_r, r)$ a function that involves the first and second derivatives of ξ_r (see its expression in SG).

The source functions, S_R and S_S, involve the dynamic properties of the turbulent medium. The expression for S_R is (see SG and Samadi et al. (2005)):

$$S_R(r,\omega_0) \quad = \quad \int_0^\infty dk \int_{-\infty}^{+\infty} d\omega\ \frac{E^2(k)}{k^2} \chi_k(\omega_0+\omega)\,\chi_k(\omega) \tag{4}$$

where k is the wavenumber, $E(k)$ the time averaged kinetic energy spectrum, $\chi_k(\omega)$ is the frequency component of $E(k,\omega)$ (the kinetic energy spectrum as a function of k and ω). A similar expression is derived for S_S (see SG). Note that the function $\chi_k(\omega)$ can be viewed as a measure in the Fourier domain of the time-correlation between eddies. This function is generally referred as 'eddy time-correlation' function.

The derivation of Eqs. (1)-(4) is based on several assumptions and approximations. Among them, the main ones are:

- *quasi-Normal approximation (QNA)*: the fourth-order moments involving the turbulent velocity are decomposed in terms of second-order ones assuming the QNA, i.e. assuming that turbulent quantities are distributed according to a Normal distribution with zero mean. However, as shown recently by Belkacem et al. (2006a), the presence of plumes causes a severe departure from this approximation. Belkacem et al. (2006a) have proposed an improved closure model that takes the asymmetry between plumes and granules as well as the turbulence inside the plumes into account. As shown by Belkacem et al. (2006b), this improved closure model reduces the discrepancy between theoretical calculations and the helioseismic constraints.

- *isotropic, homogeneous, incompressible turbulence*: the turbulent medium is assumed to be isotropic, homogeneous, and incompressible at the length scale associated with the contributing eddies. This assumption is justified for low turbulent Mach number, M_t (see SG). However, when the anisotropy is small, it is possible to apply a correction that takes the departure from isotropy into account. Such corrections have been proposed by SG and CHE in two different ways. However, in both formalisms, the exact domain over which these corrections are valid is unknown and remains to be specified.

- *radial formalism*: radial modes are usually considered. However, generalizations to non-radial modes have been proposed by Dolginov & Muslimov (1984), GMK and Belkacem et al. (2008).

- *passive scalar assumption*: as pointed out above the entropy fluctuations are supposed to behave as a passive scalar (see the discussion).

- *length-scale separation*: eddies contributing to the driving are supposed to have a characteristic length scale smaller than the mode wavelength. This assumption is justified for low M_t (see SG and the discussion).

Eddy time-correlation

Most of the theoretical formulations explicitly or implicitly assume a Gaussian function for $\chi_k(\omega)$ (GK; Dolginov & Muslimov, 1984; GMK; Balmforth, 1992; CHE). However, hydrodynamical 3D simulations of the outer layers of the Sun show that, at the length associated with the energy bearing eddies, χ_k is rather Lorentzian (Samadi et al., 2003). As pointed out by CHE, a Lorentzian χ_k is also a result predicted for the largest, most-energetic eddies by the time-dependent mixing-length formulation of convection by Gough (1977). Therefore, there are some numerical and theoretical evidences that χ_k is rather Lorentzian at the length scale of the energy bearing eddies.

The excitation of the low-frequency modes ($\nu \lesssim 3$ mHz) is mainly due to the large scales. However, the higher the frequency the more important the contribution of the small scales. Solar 3D simulations show that, at small scales, χ_k is neither Lorentzian nor Gaussian (Georgobiani et al., 2006). Then, according to Georgobiani et al. (2006), it is impossible to separate the spatial component $E(k)$ from the temporal component at all scales with the same simple analytical functions. However, such results are obtained using Large Eddy

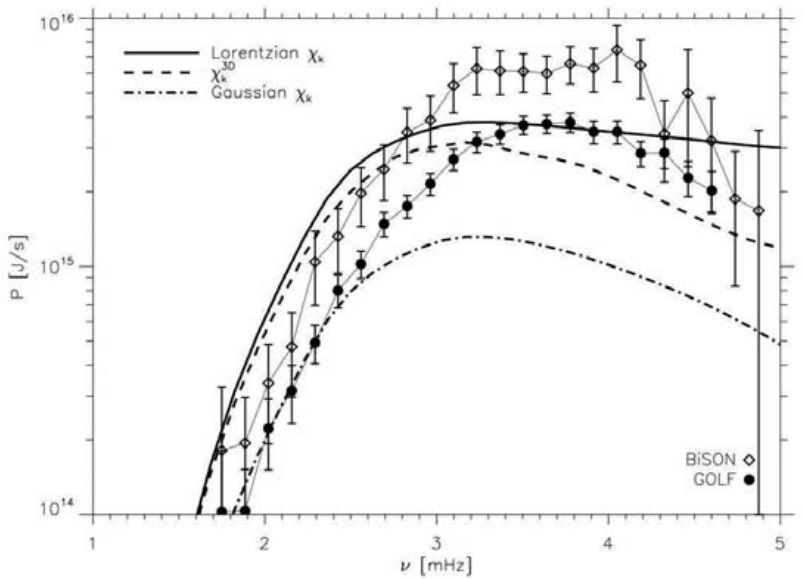

Figure 1: Solar p-mode excitation rates, $\mathcal{P}$, as a function of $\nu = \omega/2\pi$. The dots correspond to seismic data from SOHO/Golf (filled circles) and from the BiSON network (diamonds). The thick lines correspond to semi-theoretical calculations based on different choices for χ_k: Lorentzian χ_k (solid line), χ_k^{3D} i.e. χ_k directly derived from the solar 3D simulation (dashed line), and a Gaussian χ_k (dot-dashed line).

Simulation (LES). The way the small scales are treated in LES can affect our description of turbulence. Indeed, He et al. (2002) have shown that LES results in a $\chi_k(\omega)$ that decreases at all resolved scales too rapidly with ω with respect to direct numerical simulations (DNS). Moreover, Jacoutot et al. (2008a) found that computed mode excitation rates significantly depend on the adopted sub-grid model. Furthermore, at a given length scale, Samadi et al. (2007) have shown that χ_k tends toward a Gaussian when the spatial resolution is decreased. As a conclusion the numerical resolution or the sub-grid model can substantially affect our description of the small scales.

As shown by Samadi et al. (2003), calculation of the mode excitation rates based on a Gaussian χ_k results for the Sun in a significant under-estimation of the maximum of $\mathcal{P}$ whereas a better agreement with the observations is found when a Lorentzian χ_k is used (see Fig. 1). A similar conclusion is reached by Samadi et al. (2008a) in the case of the star α Cen A.

Up to now, only analytical functions were assumed for $\chi_k(\omega)$. We have here implemented, for the calculation of $\mathcal{P}$, the eddy time-correlation function derived *directly* from long time series of 3D simulation realizations with an intermediate horizontal resolution ($\simeq$ 50 km). As shown in Fig. 1, the mode excitation rates, $\mathcal{P}$, obtained from χ_k^{3D}, are found comparable to that obtained assuming a Lorentzian one, except at high frequency. This is obviously the direct consequence of the fact that a Lorentzian χ_k reproduces rather well χ_k^{3D}, except at high frequency where χ_k^{3D} decreases more rapidly than the Lorentzian function. At high frequency, calculations based on a Lorentzian χ_k result in larger $\mathcal{P}$ and reproduce better the helioseismic constraints than those based on χ_k^{3D}. This indicates perhaps that χ_k^{3D} decreases too rapidly

with frequency than it should do. This is consistent with He et al. (2002)'s results who found that LES predicts a too rapid decrease with ω compared to the DNS (see above).

CHE also found that the use of a Gaussian χ_k severely under-estimates the observed solar mode excitation rates. However, in contrast with Samadi et al. (2003), they mention that a Lorentzian χ_k results in an over-estimation for the low-frequency modes. They explain this by the fact that, at a given frequency, a Lorentzian χ_k decreases too slowly with depth compared to a Gaussian χ_k. Consequently, for the low-frequency modes, a substantial fraction of the integrand of Eq. (2) arises from large eddies situated deep in the Sun. This might suggests that, in the deep layers, the eddies that contribute efficiently have rather a Gaussian χ_k (see the discussion below).

Impact of the surface metal abundance

We have computed two 3D hydrodynamical simulations representative – in effective temperature and gravity – of the surface layers of HD 49933, a star which is rather metal poor compared to the Sun. One 3D simulation (hereafter labeled as S0) has a solar metal abundance and one other (hereafter labeled as S1) has a surface iron-to-hydrogen abundance, [Fe/H], ten times smaller. For each 3D simulation we match in the manner of Samadi et al. (2008a) an associated global 1D model and we compute the associated acoustic modes.

The rates $\mathcal{P}$ at which energy is supplied into the acoustic modes associated with S1 are found about three times smaller than those associated with S0. This difference is related to the fact that a low surface metallicity implies surface layers with a higher mean surface density. In turn, higher mean surface density implies smaller convective velocity and hence a less efficient driving of the acoustic modes (for details see Samadi et al., 2008b). This result illustrates the importance of taking the metallicity of the star into account when computing $\mathcal{P}$. This conclusion is qualitatively consistent with that by Houdek et al. (1999) who – on the basis of a mixing-length approach – also found that the mode amplitudes decrease with decreasing metal abundance.

Discussion and perspectives

The way mode excitation by turbulent convection is modeled is still very simplified. Some approximations must be improved, some assumptions or hypothesis must be avoided:

- *length-scale separation*: This approximation is less valid in the super-adiabatic region where the turbulent Mach number is no longer small (for the Sun M_t is up to 0.3). This spatial separation can however be avoided if the kinetic energy spectrum associated with the turbulent elements ($E(k)$) is properly coupled with the spatial dependence of the modes

- *eddy time-correlation function, χ_k:* Current models assume that χ_k varies with ω in the same way at any length scales and in any parts of the convective zone (CZ). At the length scale of the energy bearing eddy and in the uppermost part of the CZ, there are some strong evidences that χ_k is Lorentzian rather than Gaussian. However, as discussed here, it is not yet clear what is the correct description for χ_k at the small scales and also deep in the CZ. Use of more realistic 3D simulations would be very helpful to depict the correct dynamical behavior of the small scales as well as in the deep CZ.

- *passive scalar assumption*: This is a *strong hypothesis* that probably is no longer valid in the super-adiabatic part of the convective zone where the driving by the entropy is important. Indeed, the super-adiabatic layer is the seat of important radiative losses

by the eddies. Assuming that the entropy behaves as a passive scalar is not correct. To avoid this assumption, one needs to include eddy radiative losses in the model of stochastic excitation.

Finally, we stress that some solar-like pulsators are young stars that show a strong activity (e.g. HD 49933) which is often linked to the presence of strong magnetic fields. A strong magnetic field can inhibit convection (see e.g. Proctor & Weiss, 1982; Vögler et al., 2005). Furthermore, using 3D solar simulations, Jacoutot et al. (2008b) have studied the influence of magnetic fields of various strength on the convective cells and on the excitation mechanism. They found that a strong magnetic field results in turbulent motions of smaller scales and higher frequencies than in the absence of magnetic field, and consequently in a less efficient mode driving. Further theoretical developments are required to take the effects of a magnetic field into account in the theoretical calculation of the mode excitation rates.

Acknowledgments. RS is grateful to the SOC for the invitation to this workshop and acknowledges HELAS for the financial support.

References

Balmforth, N. J. 1992, MNRAS, 255, 639

Bedding, T. R. & Kjeldsen, H. 2007, CoAst, 150, 106

Belkacem, K., Samadi, R., Goupil, M.-J., & Dupret, M.-A. 2008, A&A, 478, 163

Belkacem, K., Samadi, R., Goupil, M. J., & Kupka, F. 2006a, A&A, 460, 173

Belkacem, K., Samadi, R., Goupil, M. J., et al. 2006b, A&A, 460, 183

Chaplin, W. J., Houdek, G., Elsworth, Y., et al. 2005, MNRAS, 360, 859 (CHE)

Dolginov, A. Z. & Muslimov, A. G. 1984, Ap&SS, 98, 15

Georgobiani, D., Stein, R. F., & Nordlund, Å. 2006, ASPC, Vol. 354, 109

Goldreich, P. & Keeley, D. A. 1977, ApJ, 212, 243 (GK)

Goldreich, P., Murray, N., & Kumar, P. 1994, ApJ, 424, 466 (GMK)

Gough, D. O. 1977, ApJ, 214, 196

He, G.-W., Rubinstein, R., & Wang, L.-P. 2002, PhFl, 14, 2186

Houdek, G., Balmforth, N. J., Christensen-Dalsgaard, J., & Gough, D. O. 1999, A&A, 351, 582

Jacoutot, L., Kosovichev, A. G., Wray, A. A., & Mansour, N. N. 2008a, ApJ, 682, 1386

Jacoutot, L., Kosovichev, A. G., Wray, A., & Mansour, N. N. 2008b, ApJ, 684, L51

Libbrecht, K. G. 1988, ApJ, 334, 510

Proctor, M. R. E. & Weiss, N. O. 1982, RPPh, 45, 1317

Samadi, R. & Goupil, M. . 2001, A&A, 370, 136 (SG)

Samadi, R., Nordlund, Å., Stein, R. F., et al. 2003, A&A, 404, 1129

Samadi, R., Goupil, M.-J., Alecian, E., et al. 2005, ApA, 26, 171

Samadi, R., Georgobiani, D., Trampedach, R., et al. 2007, A&A, 463, 297

Samadi, R., Belkacem, K., Goupil, M. J., et al. 2008a, A&A, 489, 291

Samadi, R., Ludwig, H., Belkacem, K., et al. 2008b, A&A, submitted

Vögler, A., Shelyag, S., Schüssler, M., et al. 2005, A&A, 429, 335

DISCUSSION

Houdek: The scaling law $(L/M)^{1.5}$ in Houdek et al. (1999) refers to amplitudes at the photosphere. At the height of $h = 200$ km, we obtained the $(L/M)^{1.1}$ law.

Bruntt: You find that low metallicity implies low pulsation amplitudes for solar-like oscillations. Have you tried to include metallicity as a parameter in your scaling relation of amplitudes?

Samadi: The scaling law $(L/M)^{0.7}$ proposed in Samadi et al. (2007) was indeed derived using stellar 3D simulations with solar metal abundances. Part of the remaining discrepancies between the scaling law $(L/M)^{0.7}$ and the observations may be explained by the fact that some stars have a metal abundance significantly different to that of the Sun. This is particularly so for HD 49933.

Noels: You talked about "solar" abundances. What abundances and metallicity are you refering to?

Samadi: We have considered both the "old" and the "new" solar abundances. At fixed [Fe/H], the "new" solar abundances result in a lower total metal abundance than the "old" ones and hence in lower $\mathcal{P}$. In the case of HD 49933, mode excitation rates, $\mathcal{P}$, computed by assuming the "new" solar abundances are found $\sim$ 30 % smaller than those computed assuming the "old" solar abundances (see Samadi et al., 2008b).

Noels: Could we have some solar-like oscillations in stars as massive as β Cepheid stars if a convection zone appears near the surface due to an accumulation of iron ?

Samadi: As far as we have a surface convective envelope, it is potentially possible to excite p modes. However, the excitation is efficient when the characteristic eddy turn-over time is of the same order than the period of the p modes confined near the surface.

Günter Houdek enjoying the boat ride

Comm. in Asteroseismology
Vol. 157, 2008, Wrocław HELAS Workshop 2008
M. Breger, W. Dziembowski, & M. Thompson, eds.

The effect of convection on pulsational stability

G. Houdek

Institute of Astronomy, University of Cambridge, Cambridge CB30HA, UK

Abstract

A review on the current state of mode physics in classical pulsators is presented. Two, currently in use, time-dependent convection models are compared and their applications on mode stability are discussed with particular emphasis on the location of the Delta Scuti instability strip.

Introduction

Stars with relatively low surface temperatures show distinctive envelope convection zones which affect mode stability. Among the first problems of this nature was the modelling of the red edge of the classical instability strip (IS) in the Hertzsprung-Russell (H-R) diagram. The first pulsation calculations of classical pulsators without any pulsation-convection modelling predicted red edges which were much too cool and which were at best only neutrally stable. What follows were several attempts to bring the theoretically predicted location of the red edge in better agreement with the observed location by using time-dependent convection models in the pulsation analyses (Dupree 1977; Baker & Gough 1979; Gonzi 1982; Stellingwerf 1984). More recently several authors, e.g. Bono et al. (1995, 1999), Houdek (1997, 2000), Xiong & Deng (2001, 2007), Dupret et al. (2005) were successful to model the red edge of the classical IS. These authors report, however, that different physical mechanisms are responsible for the return to stability. For example, Bono et al. (1995) and Dupret et al. (2005) report that it is mainly the convective heat flux, Xiong & Deng (2001) the turbulent viscosity, and Baker & Gough (1979) and Houdek (2000) predominantly the momentum flux (turbulent pressure p_t) that stabilizes the pulsation modes at the red edge.

Time-dependent convection models

The authors mentioned in the previous section used different implementations for modelling the interaction of the turbulent velocity field with the pulsation. In the past various time-dependent convection models were proposed, for example, by Schatzman (1956), Gough

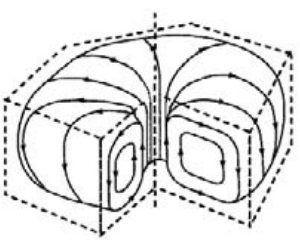

Figure 1: Sketch of an overturning hexagonal (dashed lines) convective cell. Near the centre the gas raises from the hot bottom to the cooler top (surface) where it moves nearly horizontally towards the edges, thereby loosing heat. The cooled gas then descends along the edges to close the circular flow. Arrows indicate the direction of the flow pattern.

Table 1: Summary of time-dependent convection model differences.

Balance between buoyancy & turbulent drag (Unno 1967, 1977)	Kinetic theory of accelerating eddies (Gough 1965, 1977a)
- acceleration terms of convective fluctuations w, T' neglected	- acceleration terms included: w, T' evolve with growth rate σ
- nonlinear terms approximated by spatial gradients $\propto 1/\ell$	- nonlinear terms are neglected during eddy growth
- characteristic eddy lifetime: $\tau \simeq \ell/2w$	- $\tau = 2/\sigma$ determined stochastically from parametrized shear instability
- variation $\ell_1 = \delta\ell/\ell$ (Unno 1967): $\omega\tau < 1: \ \ell_1 \sim H_1$ $\omega\tau > 1: \ \ell_1 \sim r_1$ or (Unno 1977): $\ell_1 \sim (1 + \mathrm{i}\omega^2\tau^2)^{-1}(H_1 - \mathrm{i}\omega\tau\rho_1/3)$ (H is pressure scale height)	- variation of mixing length according to rapid distortion theory (Townsend 1976), i.e. variation also of eddy shape
- turbulent pressure p_t neglected in hydrostatic support equation	- $p_\mathrm{t} = \overline{\rho}\,\overline{ww}$ included in mean equ. for hydrostatic support

(1965, 1977a), Unno (1967, 1977), Xiong (1977, 1989), Stellingwerf (1982), Kuhfuß (1986), Canuto (1992), Gabriel (1996), Grigahcène et al. (2005). Here I shall briefly review and compare the basic concepts of two, currently in use, convection models. The first model is that by Gough (1977a,b), which has been used, for example, by Baker & Gough (1979), Balmforth (1992) and by Houdek (2000). The second model is that by Unno (1967, 1977), upon which the generalized models by Gabriel (1996) and Grigahcène et al. (2005) are based, with applications by Dupret et al. (2005).

Nearly all of the time-dependent convection models assume the Boussinesq approximation to the equations of motion. The Boussinesq approximation relies on the fact that the height of the fluid layer is small compared with the density scale height. It is based on a careful scaling argument and an expansion in small parameters (Spiegel & Veronis 1960; Gough 1969). The fluctuating convection equations for an inviscid Boussinesq fluid in a static plane-parallel atmosphere are

$$\partial_t u_i + (u_j\partial_j u_i - \overline{u_j\partial_j u_i}) = -\overline{\rho}^{-1}\partial_i p' + g\widehat{\alpha}T'\,\delta_{i3}\,, \tag{1}$$

$$\partial_t T' + (u_j\partial_j T' - \overline{u_j\partial_j T'}) = \beta w - (\overline{\rho}\,\overline{c_\mathrm{p}})^{-1}\partial_i F_i'\,, \tag{2}$$

supplemented by the continuity equation for an incompressible gas, $\partial_j u_j{=}0$, where $\mathbf{u}{=}(u, v, w)$ is the turbulent velocity field, ρ is density, p is gas pressure, g is the acceleration due to gravity, T is temperature, c_p is the specific heat at constant pressure, $\widehat{\alpha} = -\overline{(\partial \ln\rho/\partial \ln T)_p}\,/\,\overline{T}$, F_i is the radiative heat flux, β is the superadiabatic temperature gradient and δ_{ij} is the Kronecker delta. Primes ($'$) indicate Eulerian fluctuations and overbars horizontal averages. These are the starting equations for the two physical pictures describing the motion of an overturning convective eddy, illustrated in Fig. 1.

In the first physical picture, adopted by Unno (1967), the turbulent element, with a characteristic vertical length ℓ, evolves out of some chaotic state and achieves steady motion very quickly. The fluid element maintains exact balance between buoyancy force and turbulent drag by continuous exchange of momentum with other elements and its surroundings. Thus the acceleration terms $\partial_t u_i$ and $\partial_t T'$ are neglected and the nonlinear advection terms provide

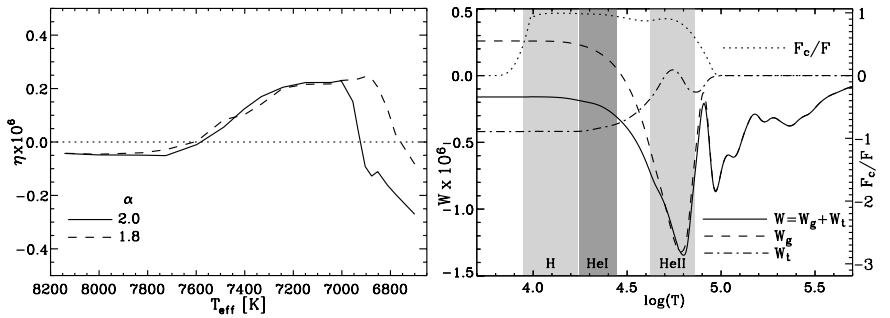

Figure 2: Mode stability of an 1.7 $M_\odot$ Delta Scuti star computed with Gough's (1977a,b) convection model. Left: Stability coefficient $\eta = \omega_i/\omega_r$ as a function of surface temperature $T_{\rm eff}$ across the IS. Results are shown for the fundamental radial mode ($n = 1$) and for two values of the mixing-length parameter α. Positive η values indicate mode instability. Right: Integrated work integral W as a function of the depth co-ordinate $\log(T)$ for a model lying just outside the cool edge of the IS ($T_{\rm eff} = 6813$ K). Results are plotted in units of η and for $\alpha = 2.0$. Contributions to W (solid curve) arising from the gas pressure perturbation, $W_{\rm g}$ (dashed curve), and the turbulent pressure fluctuations, $W_{\rm t}$ (dot-dashed curve), are indicated ($W = W_{\rm g} + W_{\rm t}$). The dotted curve is the ratio of the convective to the total heat flux $F_{\rm c}/F$. Ionization zones of H and He (5% to 95% ionization) are indicated (from Houdek 2000).

dissipation (of kinetic energy) that balances the driving terms. The nonlinear advection terms are approximated by $u_j\partial_j u_i - \overline{u_j\partial_j u_i} \simeq 2w^2/\ell$ and $u_j\partial_j T' - \overline{u_j\partial_j T'} \simeq 2wT'/\ell$. This leads to two nonlinear equations which need to be solved numerically together with the mean equations of the stellar structure.

The second physical picture, which was generalized by Gough (1965, 1977a,b) to the time-dependent case, interprets the turbulent flow by indirect analogy with kinetic gas theory. The motion is not steady and one imagines the convective element to accelerate from rest followed by an instantaneous breakup after the element's lifetime. Thus the nonlinear advection terms are neglected in the convective fluctuation equations (1)-(2) but are taken to be responsible for the creation and destruction of the convective eddies (Gough 1977a,b). By retaining only the acceleration terms the equations become linear with analytical solutions $w \propto \exp(\sigma t)$ and $T' \propto \exp(\sigma t)$ subject to proper periodic spatial boundary conditions, where t is time and $\Re(\sigma)$ is the linear convective growth rate. The mixing length ℓ enters in the calculation of the eddy's survival probability, which is proportional to the eddy's internal shear (rms vorticity), for determining the convective heat and momentum fluxes. Although the two physical pictures give the same result in a static envelope, the results for the fluctuating turbulent fluxes in a pulsating star are very different (Gough 1977a). The main differences between Unno's and Gough's convection model are summarized in Table 1.

Application on mode stability in δ Scuti stars

Fig. 2 displays the mode stability of an evolving 1.7 $M_\odot$ Delta Scuti star crossing the IS. The results were computed with the time-dependent, nonlocal convection model by Gough (1977a,b). As demonstrated in the right panel of Fig. 2, the dominating damping term to the work integral W for a star located near the red edge is the contribution from the turbulent pressure fluctuations $W_{\rm t}$.

Gabriel (1996) and more recently Grigahcène et al. (2005) generalized Unno's time-dependent convection model for stability computations of nonradial oscillation modes. They included in their mean thermal energy equation the viscous dissipation of turbulent kinetic energy, ϵ, as an additional heat source. The dissipation of turbulent kinetic energy is introduced in the conservation equation for the turbulent kinetic energy $K := \overline{u_i u_i}/2$

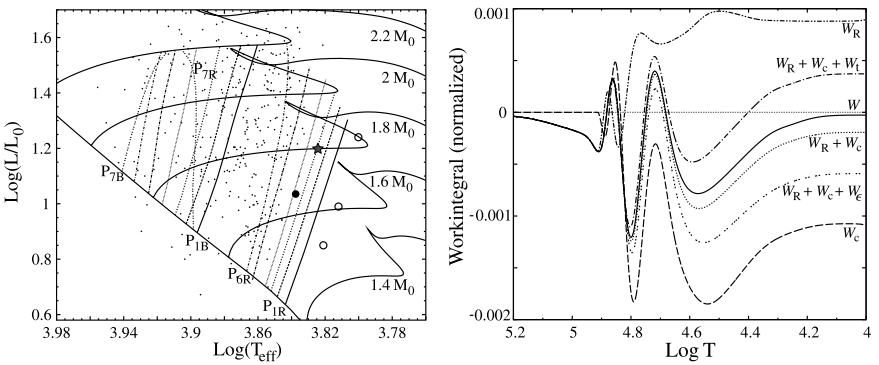

Figure 3: Stability computations of Delta Scuti stars which include the viscous dissipation rate ϵ of turbulent kinetic energy according to Grigahcène et al. (2005). Left: Blue and red edges of the IS superposed on evolutionary tracks on the theorists H-R diagram. The locations of the edges, labelled p_{nB} and p_{nR}, are indicated for radial modes with orders $1 \leq n \leq 7$. Results by Houdek (2000, $\alpha = 2.0$, see Fig. 2) and Xiong & Deng (2001) for the gravest p modes are plotted as the filled and open circles respectively. Right: Integrated work integral W as a function of the depth co-ordinate $\log(T)$ for a stable $n = 3$ radial mode of a $1.8\,M_\odot$ star (see 'star' symbol in the left panel). Contributions to W arising from the radiative flux, W_R, the convective flux, W_c, the turbulent pressure fluctuations, W_t ($W_R + W_c + W_t$), and from the perturbation of the turbulent kinetic energy dissipation, W_ϵ ($W_R + W_c + W_\epsilon$), are indicated (adapted from Dupret et al. 2005).

(e.g. Tennekes & Lumley 1972, §3.4; Canuto 1992; Houdek & Gough 1999):

$$D_t K + \partial_j(\overline{K u_j} + \overline{\rho}^{-1}\overline{p' u_j}) - \nu\partial_i^2 K = -\overline{u_i u_j}\partial_j U_i + g\widehat{\alpha}\overline{u_j T'} - \epsilon\,, \tag{3}$$

where D_t is the material derivative, U_i is the average (oscillation) velocity, i.e. the total velocity $\tilde{u}_i = U_i + u_i$, and ν is the constant kinematic viscosity (in the limit of high Reynolds numbers the molecular transport term can be neglected). The first and second term on the right of Eq. (3) are the shear and buoyant productions of turbulent kinetic energy, whereas the last term $\epsilon = \nu\overline{(\partial_j u_i + \partial_i u_j)^2}/2$ is the viscous dissipation of turbulent kinetic energy into heat. This term is also present in the mean thermal energy equation, but with opposite sign. The linearized perturbed mean thermal energy equation for a star pulsating radially with complex angular frequency $\omega = \omega_r + i\omega_i$ can then be written, in the absence of nuclear reactions, as ('δ' denotes a Lagrangian fluctuation and I omit overbars in the mean quantities):

$$d\delta L/dm = -i\omega c_p T(\delta T/T - \nabla_{ad}\delta p/p) + \delta\epsilon\,, \tag{4}$$

where m is the radial mass co-ordinate, $\nabla_{ad} = (\partial \ln T/\partial \ln p)_s$ and L is the total (radiative and convective) luminosity. Grigahcène et al. (2005) evaluated ϵ from a turbulent kinetic energy equation which was derived without the assumption of the Boussinesq approximation. Furthermore it is not obvious whether the dominant buoyancy production term, $g\widehat{\alpha}\overline{u_j T'}$ (see Eq. 3), was included in their turbulent kinetic energy equation and so in their expression for ϵ.

Dupret et al. (2005) applied the convection model of Grigahcène et al. (2005) to Delta Scuti and γ Doradus stars and reported well defined red edges. The results of their stability analysis for Delta Scuti stars are depicted in Fig. 3. The left panel compares the location of the red edge with results reported by Houdek (2000, see also Fig. 2) and Xiong & Deng (2001). The right panel of Fig. 3 displays the individual contributions to the accumulated work integral W for a star located near the red edge of the $n = 3$ mode (indicated by the 'star'

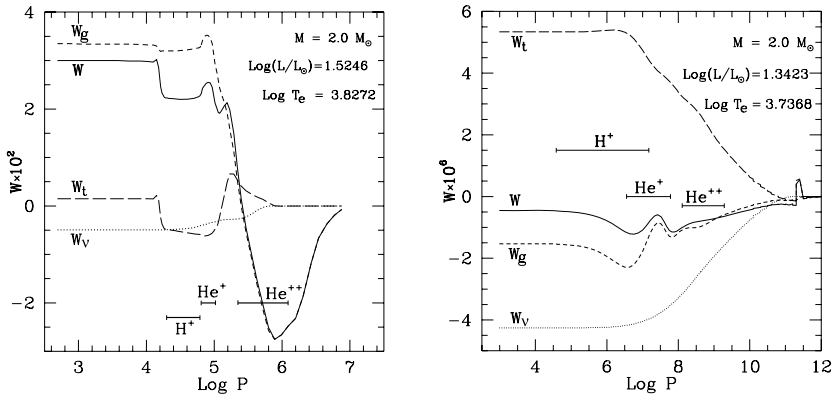

Figure 4: Accumulated work integral W as a function of the depth co-ordinate $\log(p)$. Results are shown for the $n = 1$ radial mode of a Delta Scuti star located inside the IS (left panel) and outside the red edge of the IS (right panel). The stability calculations include viscous dissipation by the small-scale turbulence (Xiong 1989; see Eq. 6). Contributions to W (solid curve) arising from the fluctuating gas pressure, $W_{\rm g}$ (dashed curve), the turbulent pressure perturbations, $W_{\rm t}$ (long-dashed curve), and from the turbulent viscosity, W_ν (dotted curve), are indicated ($W = W_{\rm g} + W_{\rm t} + W_\nu$). The ionization zones of H and He are marked (adapted from Xiong & Deng 2007).

symbol in the left panel). It demonstrates the near cancellation effect between the contributions of the turbulent kinetic energy dissipation , W_ϵ, and turbulent pressure, $W_{\rm t}$, making the contribution from the fluctuating convective heat flux, $W_{\rm c}$, the dominating damping term. The near cancellation effect between W_ϵ and $W_{\rm t}$ was demonstrated first by Ledoux & Walraven (1958, §65) (see also Gabriel 1996) by writing the sum of both work integrals as:

$$W_\epsilon + W_{\rm t} = 3\pi/2 \int_{m_{\rm b}}^{M} (5/3 - \gamma_3) \Im(\delta p_{\rm t}^* \delta\rho) \rho^{-2} \, {\rm d}m \,, \tag{5}$$

where M is the stellar mass, $m_{\rm b}$ is the enclosed mass at the bottom of the envelope and $\gamma_3 \equiv 1 + (\partial \ln T/\partial \ln \rho)_s$ (s is specific entropy) is the third adiabatic exponent. Except in ionization zones $\gamma_3 \simeq 5/3$ and consequently $W_\epsilon + W_{\rm t} \simeq 0$.

The convection model by Xiong (1977, 1989) uses transport equations for the second-order moments of the convective fluctuations. In the transport equation for the turbulent kinetic energy Xiong adopts the approximation by Hinze (1975) for the turbulent dissipation rate, i.e. $\epsilon = 2\chi k(\overline{u_i u_i}\rho^2/3\overline{\rho^2})^{3/2}$, where $\chi = 0.45$ is the Heisenberg eddy coupling coefficient and $k \propto \ell^{-1}$ is the wavenumber of the energy-containing eddies. However, Xiong does not provide a work integral for ϵ (neither does Unno et al. 1989, §26,30) but includes the viscous damping effect of the small-scale turbulence in his model. The convection models considered here describe only the largest, most energy-containing eddies and ignore the dynamics of the small-scale eddies lying further down the turbulent cascade. Small-scale turbulence does, however, contribute directly to the turbulent fluxes and, under the assumption that they evolve isotropically, they generate an effective viscosity $\nu_{\rm t}$ which is felt by a particular pulsation mode as an additional damping effect. The turbulent viscosity can be estimated as (e.g. Gough 1977b; Unno et al. 1989, §20) $\nu_{\rm t} \simeq \lambda(\overline{ww})^{1/2}\ell$, where λ is a parameter of order unity. The associated work integral W_ν can be written in Cartesian co-ordinates as (Ledoux & Walraven 1958, §63)

$$W_\nu = -2\pi\,\omega_\mathrm{r} \int_{m_\mathrm{b}}^{M} \nu_\mathrm{t} \left[e_{ij} e_{ij} - \frac{1}{3} \left(\nabla \cdot \boldsymbol{\xi} \right)^2 \right] \mathrm{d}m\,, \tag{6}$$

where $e_{ij} = (\partial_j \xi_i + \partial_i \xi_j)/2$ and $\boldsymbol{\xi}$ is the displacement eigenfunction. Xiong & Deng (2001, 2007) modelled successfully the IS of Delta Scuti and red giant stars and found the dominating damping effect to be the turbulent viscosity (Eq. 6). This is illustrated in Fig. 4 for two Delta Scuti stars: one is located inside the IS (left panel), the other outside the cool edge of the IS (right panel). The contribution from the small-scale turbulence was also the dominant damping effect in the stability calculations by Xiong et al. (2000) of radial p modes in the Sun, although the authors still found unstable modes with orders between $11 \leq n \leq 23$. The importance of the turbulent damping was reported first by Goldreich & Keeley (1977) and later by Goldreich & Kumar (1991), who found all solar modes to be stable only if turbulent damping was included in their stability computations. In contrast, Balmforth (1992), who adopted the convection model of Gough (1977a,b), found all solar p modes to be stable due mainly to the damping of the turbulent pressure perturbations, W_t, and reported that viscous damping, W_ν, is about one order of magnitude smaller than the contribution of W_t. Turbulent viscosity (Eq. 6) leads always to mode damping, where as the perturbation of the turbulent kinetic energy dissipation, $\delta\epsilon$ (see Eq. 4), can contribute to both damping and driving of the pulsations (Gabriel 1996). The driving effect of $\delta\epsilon$ was shown by Dupret et al. (2005) for a γ Doradus star.

Summary

We discussed three different mode stability calculations of Delta Scuti stars which successfully reproduced the red edge of the IS. Each of these computations adopted a different time-dependent convection description. The results were discussed by comparing work integrals. All convection descriptions include, although in different ways, the perturbations of the turbulent fluxes. Gough (1977a), Xiong (1977, 1989), and Unno et al. (1989) did not include the contribution W_ϵ to the work integral because in the Boussinesq approximation (Spiegel & Veronis 1960) the viscous dissipation is neglected in the thermal energy equation. In practise, however, this term may be important. Grigahcène et al. (2005) included W_ϵ but ignored the damping contribution of the small-scale turbulence W_ν, which was found by Xiong & Deng (2001, 2007) to be the dominating damping term. The small-scale damping effect was also ignored in the calculations by Houdek (2000). A more detailed comparison of the convection descriptions has not yet been made but Houdek & Dupret have begun to address this problem.

Acknowledgments. I am grateful to Douglas Gough for helpful discussions and to the HELAS organizing committee for travel support. Support by the UK Science and Technology Facilities Council is acknowledged.

References

Baker, N., & Gough, D. O. 1979, ApJ, 234, 232

Balmforth, N. J. 1992, MNRAS, 255, 603

Bono, G., Caputo, F., Castellani, V., et al. 1995, ApJ, 442, 159

Bono, G., Marconi, M., & Stellingwerf, R. 1999, ApJSS, 122, 167

Canuto, V. 1992, ApJ, 392, 218

Dupree, R. G. 1977, ApJ, 215, 232

Dupret, M.-A., Grigahcène, A., Garrido, R., et al. 2005, A&A, 435, 927

Gabriel, M. 1996, BASI, 24, 233

Goldreich, P., & Keeley, D. A. 1977, ApJ, 211, 934

Goldreich, P., & Kumar, P. 1991, ApJ, 374, 366

Gonzi, G. 1982, A&A, 110, 1

Gough, D. O. 1965, in Geophys. Fluid Dynamics, Woods Hole Oceanographic Institutions, Vol. 2, Woods Hole, Mass., p. 49

Gough, D. O. 1969, JAtS, 26, 448

Gough, D. O. 1977a, ApJ, 214, 196

Gough, D. O. 1977b, in Problems of Stellar Convection, Spiegel E.A., Zahn J.-P., eds, Springer-Verlag, Berlin, p. 15

Grigahcène, A., Dupret, M.-A., Gabriel, M., et al. 2005, A&A, 434, 1055

Hinze, J. O. 1975, Turbulence, McGraw-Hill, New York

Houdek, G. 1997, in Proc. IAU Symp. 181: Sounding Solar and Stellar Interiors, Schmider F.-X., Provost J., eds, Nice Observatory, p. 227

Houdek, G. 2000, in Delta Scuti and Related Stars, Breger M., Montgomery M.H., eds, ASP Conf. Ser., Vol. 210, Astron. Soc. Pac., San Francisco, p. 454

Houdek, G., & Gough, D.O. 1999, in Theory & Tests of Convection in Stellar Structure, Guinan E.F., Montesinos B., eds, ASP Conf. Ser. 173, San Francisco, p. 237

Kuhfuß R. 1986, A&A, 160, 116

Ledoux, P., & Walraven, T. 1958, in Handbuch der Physik, Vol. LI, Flügge S., ed., Springer-Verlag, Berlin, p. 353

Schatzman, E. 1956, AnAp, 19, 51

Spiegel, E. A., & Veronis, G. 1960, ApJ, 131, 442 (correction: ApJ, 135, 665)

Stellingwerf, R. F. 1982, ApJ, 262, 330

Stellingwerf, R. F. 1984, ApJ, 284, 712

Tennekes, H., & Lumley, J. L. 1972, A First Course in Turbulence, The MIT Press

Townsend, A. A. 1976, The Structure of Turbulent Shear Flow, CUP

Unno, W. 1967, PASJ, 19, 40

Unno, W. 1977, in Problems of Stellar Convection, Spiegel E.A., Zahn J.-P., eds, Springer-Verlag, Berlin, p. 315

Unno, W., Osaki, Y., Ando, H., Saio, H, & Shibahashi, H. 1989, Nonradial Oscillations of Stars, Second Edition, University of Tokyo Press

Xiong, D. R. 1977, AcASn, 18, 86

Xiong, D. R. 1989, A&A, 209, 126

Xiong, D. R., Cheng, Q. L., & Deng, L. 2000, MNRAS, 319, 1079

Xiong, D. R., & Deng, L. 2001, MNRAS, 324, 243

Xiong, D. R., & Deng, L. 2007, MNRAS, 378, 1270

DISCUSSION

Christensen-Dalsgaard: How does the mixing length affect the red edge of the γ Dor instability strip?

Houdek: The location of the red edge is predominantly determined by radiative damping which gradually dominates over the driving effect of the so-called convective flux blocking mechanism (Dupret et al. 2005). A change in the mixing length will not only affect the depth of the envelope convection zone but also the characteristic time scale of the convection and consequently the stability of g modes with different pulsation periods. A calibration of the mixing length to match the observed location of the γ Dor instability strip will also calibrate the depth of the convection zone at a given surface temperature.

Comm. in Asteroseismology
Vol. 157, 2008, Wrocław HELAS Workshop 2008
M. Breger, W. Dziembowski, & M. Thompson, eds.

Stochastic wave excitation in rotating stars

S. Mathis[1,2], K. Belkacem[3], and M. J. Goupil[3]

[1] CEA/DSM/IRFU/SAp, Laboratoire AIM CEA/DSM, CNRS,
Université Paris Diderot, F-91191 Gif-sur-Yvette Cedex, France
[2] Observatoire de Paris, LUTH, CNRS, UMR 8102, F-92195 Meudon, France
[3] Observatoire de Paris, LESIA, CNRS, UMR 8109, F-92195 Meudon, France

Abstract

Wave propagation, excitation and associated transport are modified by the Coriolis and the centrifugal accelerations in rotating stars. In this work, we focus on the influence of the Coriolis acceleration on the volumetric stochastic excitation in convection zones of rotating stars. First, we present the complete formalism which has been derived and discuss the different terms which appear due to the Coriolis acceleration. Then, we use this formalism to compute the solar mode excitation rates and emphasize the peculiar behavior due to rotation. Consequences on wave transport in rotating stars are eventually discussed.

Introduction

The motivation of this work is to investigate the effect of uniform rotation on the stochastically excited mode amplitudes. Several issues can be addressed; is the amplitude of a non-axisymmetric mode ($m \neq 0$) the same as for an axisymmetric one ($m = 0$)? Are prograde and retrograde modes excited in the same manner and what are the consequences? This can have some important consequences from both an observational point of view as well as a theoretical one.

As a first step, we neglect the centrifugal acceleration that induces a deformation of the star. We then focus our attention on the effect of the Coriolis acceleration. We also restrict the study to uniform rotation. In the first section, we present a formalism of stochastic excitation developed for a rotating star, and we apply it to the solar case by performing a perturbative development. Some consequences on the angular momentum transport by modes are briefly discussed in a third section. Conclusion and perspectives are provided in the last section.

Physical assumptions and formalism

Following Samadi & Goupil (2001) and Belkacem et al. (2008), we establish the inhomogeneous wave equation

$$\left(\partial_{t^2} - \vec{L}_\Omega\right) \vec{v}_{\rm osc} + \vec{\mathcal{C}}(\vec{v}_{\rm osc}, \vec{u}_t) = \vec{\mathcal{S}}_t(\vec{u}_t)\,.^1 \tag{1}$$

[1] Here the following notation for partial derivatives $\frac{\partial^n f}{\partial x^n} = \partial_{x^n} f$ is adopted.

$\vec{v}_{\rm osc}$ is the velocity field of the waves and $\vec{u}_t$ is the turbulent one associated to the convective eddies. The $\vec{\mathcal{C}}(\vec{v}_{\rm osc},\vec{u}_t)$ vector field, which is not detailed here, is related to the wave-turbulence interaction that corresponds to the dynamical damping, η. $\vec{L}_\Omega$ is the operator that rules the wave dynamics in the case of the star free oscillations

$$\begin{aligned}\vec{L}_\Omega\left(\vec{v}_{\rm osc}\right) &= \vec{\nabla}\left[\alpha_s\vec{v}_{\rm osc}\cdot\vec{\nabla}s_0+c_s^2\vec{\nabla}\cdot\left(\rho_0\vec{v}_{\rm osc}\right)\right]-\vec{g}_{\rm eff}\vec{\nabla}\cdot\left(\rho_0\vec{v}_{\rm osc}\right)\\ &- \rho_0\Omega\partial_{t,\varphi}\vec{v}_{\rm osc}-2\,\rho_0\vec{\Omega}\times\partial_t\vec{v}_{\rm osc}-\rho_0 r\sin\theta\left(\partial_t\vec{v}_{\rm osc}\cdot\vec{\nabla}\Omega\right)\widehat{e}_\varphi\,. \qquad (2)\end{aligned}$$

ρ, $g_{\rm eff}$ and Ω are respectively the fluid density, effective gravity acceleration (including the centrifugal one) and angular velocity. c_s is the sound speed while $\alpha_s=\left(\partial p/\partial s\right)_\rho$, where p is the pressure and s the macroscopic entropy. X_0 and X_1 (where $X=\{\rho,p,s\}$) are respectively the hydrostatic value of X and its wave-associated fluctuation. Finally, (r,θ,φ) are the classical spherical coordinates.

The source terms that drive the eigenmodes are

$$\vec{\mathcal{S}}_t\left(\vec{u}_t\right)=\vec{\mathcal{S}}_{\rm SG}-\partial_t\left[\rho_1\left(\Omega\partial_\varphi\vec{u}_t+2\vec{\Omega}\times\vec{u}_t+r\sin\theta\left(\vec{u}_t\cdot\vec{\nabla}\Omega\right)\widehat{e}_\varphi\right)\right]\,. \qquad (3)$$

The term $\vec{\mathcal{S}}_{\rm SG}$ contains the source terms as derived by Samadi & Goupil (2001) and Belkacem et al. (2008), in which the dominant ones are the Reynolds and entropy contributions. The three last terms are those induced by rotation and can be re-expressed such as

$$\partial_t\left(2\,\rho_1\vec{\Omega}\times\vec{u}_t\right)=2\vec{\Omega}\times\partial_t\left(\rho_1\vec{u}_t\right)=-2\vec{\Omega}\times\left[\vec{\nabla}\cdot\left(\rho_0\vec{u}_t\right)\,\vec{u}_t\right] \qquad (4)$$

$$\partial_t\left(\rho_1\Omega\partial_\varphi\vec{u}_t\right)=\Omega\left[\vec{\nabla}\cdot\left(\rho_0\vec{u}_t\right)\partial_\varphi\vec{u}_t\right] \qquad (5)$$

$$\partial_t\left[\rho_1 r\,\sin\theta\left(\vec{u}_t\cdot\vec{\nabla}\Omega\right)\right]=-r\sin\theta\left[\vec{\nabla}\cdot\left(\rho_0\vec{u}_t\right)\vec{u}_t\right]\cdot\vec{\nabla}\Omega, \qquad (6)$$

where $\vec{\Omega}$ is supposed uniform and steady on a dynamical time scale. These last three terms scale as M_t^3 (M_t is the turbulent Mach number), while Samadi & Goupil (2001) have shown the Reynolds contribution scales as M_t^2. Thus the above rotational contribution can be ignored in front of the Reynolds one. Moreover, in the case where the turbulent convective motions are assumed to be anelastic ($\vec{\nabla}\cdot\left(\rho_0\vec{u}_t\right)=0$), they can be neglected. Therefore, the only source terms we must retain are the Reynolds and the entropy ones.

Following the procedure detailed by Samadi & Goupil (2001) and Belkacem et al. (2008), the power supplied into the modes (P) is derived

$$P=\left(C_R^2+C_S^2+C_c^2\right)/\left(8I\right) \qquad (7)$$

where C_R^2, C_S^2, and C_c^2 are respectively the contributions of the Reynolds stresses, of the entropy fluctuation advection, and the crossed terms. The crossed terms are ignored in front of C_R^2 and C_S^2 (see Belkacem et al. 2008 for details). In addition, as shown above the source terms related to the rotation have been neglected.

The Reynolds stresses contribution is given by

$$C_R^2=4\pi^3\int{\rm d}m\;R(r)\;S_R(\omega_0), \qquad (8)$$

where

$$S_R\left(\omega_0\right)=\int\frac{{\rm d}k}{k^2}\;E^2(k)\;\int{\rm d}\omega\;\chi_k(\omega+\omega_0)\;\chi_k(\omega)\,. \qquad (9)$$

$E(k)$ and $\chi_k(\omega)$ are respectively the kinetic energy spectrum and the temporal correlation function which are also modified through the action of rotation on turbulence. The frequencies ω_0 and ω are associated with pulsation and convection, respectively. Furthermore

$$R(r) = R_{\rm spheroidal} + R_{\rm toroidal} \tag{10}$$

$$\text{with} \quad R_{\rm toroidal} = \frac{11}{15} L^2 \left| \frac{d\xi_T}{dr} - \frac{\xi_T}{r} \right|^2 + \left| \frac{\xi_T}{r} \right|^2 \left(\frac{11}{5} L^2 (L^2-2) - \frac{8}{5} \mathcal{F}_{\ell,|m|} - \frac{2}{3} L^2 \right) \tag{11}$$

where $R_{\rm spheroidal}$ is given by Eq. (23) of Belkacem et al. (2008), $\mathcal{F}_{\ell,|m|} = \frac{|m|(2\ell+1)}{2} \left[L^2 - (m^2+1) \right]$, $L^2 = \ell(\ell+1)$, and (ξ_r, ξ_H, ξ_T) are the radial, horizontal and toroidal components of the eigenfunction corresponding to a spherical harmonic (Y_ℓ^m). $R_{\rm spheroidal}$ corresponds to the non-rotating case. It is modified by the Coriolis acceleration through the modification of ξ_r and of ξ_H it induces.

The second source term, the entropy fluctuation contribution is obtained as

$$C_S^2 = \frac{4\pi^3 \mathcal{H}}{\omega_0^2} \int \frac{{\rm d}r}{r^2} \alpha_s^2 \left(\left| D_\ell \frac{d\,(\ln \mid \alpha_s \mid)}{d \ln r} - \frac{dD_\ell}{d \ln r} \right|^2 + L^2 \mid D_\ell \mid^2 \right) \mathcal{S}_S(\omega_0) \tag{12}$$

with $\mathcal{H}$ an anisotropy factor (defined in Samadi & Goupil 2001), $D_\ell = \frac{1}{r^2} \frac{d}{dr} \left(r^2 \xi_r \right) - \frac{L^2}{r} \xi_H$ and

$$\mathcal{S}_S(\omega_0) = \int \frac{{\rm d}k}{k^4} E(k) E_s(k) \int {\rm d}\omega \, \chi_k(\omega_0 + \omega) \, \chi_k(\omega), \tag{13}$$

E_s being the spectrum associated to the entropy turbulent fluctuations. As for $R_{\rm spheroidal}$ no direct changes are due to uniform rotation.

Application to the excitation of solar oscillation modes

In this section, we apply the formalism to spheroidal solar oscillation modes for which $2\Omega/\omega_0$ (where ω_0 is (hereafter) the mode frequency in the non-rotating case) is such that they are only slightly perturbed by the Coriolis acceleration. In this case, we get respectively for each displacement eigenmode component (cf. Unno et al. 1989)

$$\xi_\alpha = \xi_\alpha^{(0)} + m \left(\frac{2\Omega}{\omega_0} \right) \xi_\alpha^{(1)} \quad \text{and} \quad \xi_T = \left(\frac{2\Omega}{\omega_0} \right) \xi_T^{(1)} \tag{14}$$

where $\alpha = \{r, H\}$, $\xi_\alpha^{(0)}$ being the component in the non-rotating case for which $\xi_T^{(0)} = 0$, and $\xi_\alpha^{(1)}$ and $\xi_T^{(1)}$ are given by Unno et al (1989).

Using these expansions in Eq. (7), we get

$$P_{n,l,m} = P_{n,l,m}^{(0)} + m \left(\frac{2\Omega}{\omega_0} \right) P_{n,l,m}^{(1)} \tag{15}$$

so that the excitation rate is different for prograde ($m < 0$) and retrograde ($m > 0$)[2] modes since it depends explicitly on m. To better quantify this bias introduced by the Coriolis acceleration, we define

$$\delta P_m / P_{-m} = (P_m - P_{-m}) / P_{-m} \tag{16}$$

[2] The mode phase is expanded as $\exp\left[i\left(m\varphi + \omega_0 t\right)\right]$.

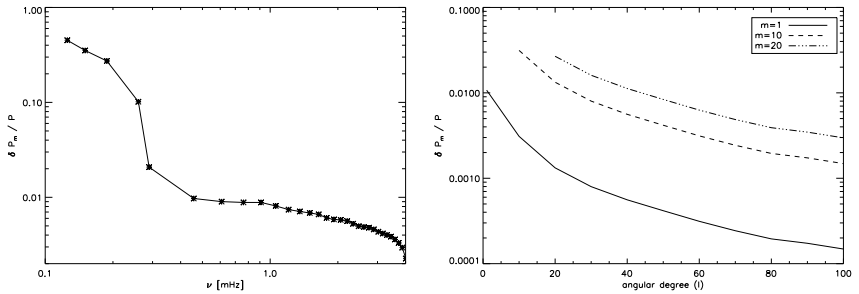

Figure 1: **Left panel:** Bias between prograde and retrograde modes (see Eq.(16)) for $\ell = 1$ modes, computed with a standard solar model. **Right panel:** Bias between prograde and retrograde modes as a function of the mode angular degree (ℓ) and for a radial order $n = 5$.

which is plotted in Fig. (1). In this first application, the simplest turbulent spectrum of Kolmogorov is assumed in evaluating Eqs (9) and (13). For low-frequency g modes that are excited in the bottom of the convection zone, where $2\Omega \approx \omega_c$ (ω_c being the convective frequency) the effect of rotation on the convective velocity field has to be taken into account (work in progress).

First, $\delta P_m/P_{-m}$ scales as $2\Omega/\omega_0$. Therefore, in the solar case, we find that acoustic mode excitation rates are only weakly affected by the Coriolis acceleration while gravity modes are affected up to 50 % for the most low-frequency modes. On the other hand, for a given m, $\delta P_m/P_{-m}$ increases for decreasing ℓ (it becomes maximum for $l = |m|$); in other words the bias is stronger for low-ℓ degrees.

Mode-induced transport

Let us now examine the mode-induced transport of angular momentum. The eulerian flux of angular momentum introduced by the Reynolds stresses, for each azimuthal order m is given by (see Lee & Saio 1993)

$$\mathcal{F}_{\mathrm{AM;m}} = \int_{4\pi} \rho_0 r \sin\theta \, u_{r;m} u^*_{\varphi;m} \mathrm{d}\widetilde{\Omega} \quad \text{where} \quad \vec{u} = i\,\omega_0\,\vec{\xi}, \tag{17}$$

$\mathrm{d}\widetilde{\Omega} = \sin\theta \mathrm{d}\theta\mathrm{d}\varphi$ being the solid angle. In the non-rotating adiabatic case, we get

$$\mathcal{F}_{\mathrm{AM;m}} + \mathcal{F}_{\mathrm{AM;-m}} = 0; \tag{18}$$

therefore, modes do not transport any net flux of angular momentum. In the rotating dissipative case, introducing Eq.(14) into Eq.(17) , we get

$$\begin{aligned} &\mathcal{F}_{\mathrm{AM;m}} + \mathcal{F}_{\mathrm{AM;-m}} = \\ &-2\mathcal{D}(\eta)\,\rho_0 r \sum_{n,l} \omega_0^2\,(2\Omega/\omega_0)\,\mathcal{I}_m\left\{ \left[A^2_{l,m}\right]^{(0)}\ \mathcal{G}_1 + \left[A^2_{l,m}\right]^{(1)}\ \mathcal{G}_2 \right\} \neq 0 \end{aligned} \tag{19}$$

where $\mathcal{I}_m$ denotes the imaginary part, and

$$\mathcal{G}_1 = \left[m^2 \left(\xi^{(1)}_{r;l} \xi^{(0)*}_{H;l} + \xi^{(0)}_{r;l} \xi^{(1)*}_{H;l} \right) + \xi^{(0)}_{r;l} \left(\alpha^m_{l-1} \xi^{(1)}_{T;l-1} - \beta^m_{l+1} \xi^{(1)}_{T;l+1} \right)^* \right] \tag{20}$$

$$\mathcal{G}_2 = -m^2\, \xi^{(0)}_{r;l} \xi^{(0)*}_{H;l} \tag{21}$$

with

$$\alpha_{\ell,m}=\ell\sqrt{\frac{(\ell+1)^2-m^2}{(2\ell+1)(2\ell+3)}} \quad \text{and} \quad \beta_{\ell,m}=(\ell+1)\sqrt{\frac{\ell^2-m^2}{(2\ell+1)(2\ell-1)}}. \tag{22}$$

$\mathcal{D}$ corresponds to the phase shift between $u_{r;m}$ and $u_{\varphi;m}$ due to dissipative processes (e.g., the thermal diffusion or the viscous friction) that causes a net transport of angular momentum (Goldreich & Nicholson 1989). Here, we assume that the damping is quasi-independent of m since $\omega_0 \gg m\,\Omega$ for the considered modes. Then, the amplitude is developed as for the power, *i.e.*

$$A^2_{\ell,m} = \left[A^2_{\ell,m}\right]^{(0)} + m\left(\frac{2\Omega}{\omega_0}\right)\left[A^2_{\ell,m}\right]^{(1)} \tag{23}$$

$$= \frac{P^{(0)}}{2\eta I\omega_0^2} + m\left(\frac{2\Omega}{\omega_0}\right)\frac{P^{(1)}}{2\eta I\omega_0^2}\,. \tag{24}$$

Therefore, the Coriolis acceleration introduces extra biases between prograde and retrograde waves through the modifications of the eigenfunctions ($\mathcal{G}_1$) and of the excitation rate ($[A^2_{l,m}]^{(1)}$).

Conclusion

In this work, we derive the formalism that allows to treat the stochastic excitation of modes by convective regions in presence of rotation. Then, we applied it, as a first application, to the solar spheroidal oscillations. We show that a bias between pro- and retrograde waves is introduced in the excitation by the Coriolis acceleration. It can be relatively important for low-frequency g-modes while it is quite negligible for acoustic ones. We showed that the azimuthal asymmetries both in eigenfunctions and their excitation rates introduce an extra contribution. The associated mode-induced transport of angular momentum remains to be quantified as in Talon & Charbonnel (2005).

Future works must apply the formalism to the case of rapid rotators for both inertial and gravito-inertial modes (Dintrans & Rieutord 2000, Rieutord et al. 2001) and include the effect of differential rotation.

References

Belkacem, K., Samadi, R., Goupil, M. J., & Dupret, M.-A. 2008, A&A, 478, 163

Dintrans, B., & Rieutord, M. 2000, A&A, 354, 86

Goldreich, P., & Nicholson, P. D. 1989, ApJ, 342, 1075

Lee, U., & Saio, H. 1993, MNRAS, 261, 415

Rieutord, M., Georgeot, B., & Valdettaro, L. 2001, JFM, 435, 103

Samadi, R., & Goupil, M. J. 2001, A&A, 370, 136

Talon, S., & Charbonnel, C. 2005, A&A, 440, 981

Unno, W., Osaki, Y., Ando, H., Saio, H., & Shibahashi, H. 1989, *Nonradial oscillations of stars*, University of Tokyo Press

DISCUSSION

Guzik: Do you see the asymmetry in excitation introduced by the Coriolis acceleration in any stellar g-mode data? Where should we look for it?

Mathis: I have not seen it yet in any data, but we have to look at this to eventually get an additional observational constraint on gravity mode behaviour.

Comm. in Asteroseismology
Vol. 157, 2008, Wrocław HELAS Workshop 2008
M. Breger, W. Dziembowski, & M. Thompson, eds.

The role of negative buoyancy in convective Cepheid models. Double-mode pulsations revisited

R. Smolec

Copernicus Astronomical Center, Bartycka 18, 00-716 Warszawa, Poland

Abstract

The longstanding problem of modeling double-mode behaviour of classical pulsators was solved with the incorporation of turbulent convection into pulsation hydrocodes. However, the reasons for the computed double-mode behaviour were never clearly identified. In our recent papers (Smolec & Moskalik 2008a,b) we showed that the double-mode behaviour results from the neglect of negative buoyancy effects in some of the hydrocodes. If these effects are taken into account, no stable nonresonant double-mode behaviour can be found. In these proceedings, we focus our attention on the role of negative buoyancy effects in classical Cepheid models.

Introduction

Since the early days of nonlinear pulsation computations, modeling double-mode (DM) phenomenon was one of the major objectives. However, the search for nonresonant double-mode behaviour with radiative hydrocodes failed (see however , Kovács & Buchler 1993). The typical modal selection observed was first overtone (1O) pulsation at the hot side of the instability strip (IS), fundamental mode (F) pulsation at the red side, and either-or domain (F/1O) in between. The incorporation of turbulent convection into pulsation hydrocodes led to stable and robust double-mode pulsation (Kolláth et al. 1998, Feuchtinger 1998). Most of the double-mode models published so far were computed with the use of the Florida-Budapest hydrocode (e.g. Kolláth et al. 2002). This hydrocode adopts a time-dependent convection model based on the Kuhfuß (1986) work. Although the Kuhfuß model was also adopted in our pulsation hydrocodes (Smolec & Moskalik 2008a), we could not find a double-mode behaviour, despite our extensive search for it (Smolec & Moskalik 2008b). We linked the difference in the computed modal selection to a different treatment of negative buoyancy effects in both codes. In the Florida-Budapest code, negative buoyancy is neglected, while it is present in our hydrocodes. The comparison of both treatments (performed with our hydrocodes) allows us to understand the reasons for double-mode behaviour computed with hydrocodes that neglect negative buoyancy.

Turbulent convection model

In the Kuhfuß model of turbulent convection, equations of motion and energy conservation are supplemented with an additional, single equation for generation of turbulent energy, e_t. Details of the model can be found e.g. in Smolec & Moskalik (2008a). Here we focus our

attention on the turbulent energy equation and its crucial terms (turbulent pressure and flux of turbulent kinetic energy neglected):

$$\frac{de_t}{dt} = S - D + E.V. \tag{1}$$

In the above equation, S is the turbulent source function (or driving function), responsible for the driving of turbulent eddies through the buoyant forces. The source function is proportional to the superadiabatic gradient, $Y = \nabla - \nabla_a$, and to the speed of convective elements, $\sim e_t^{1/2}$. The D-term models the decay of turbulent eddies, through the turbulent cascade, $D \sim e_t^{3/2}$. $E.V.$ describes energy transfer through eddy-viscous forces. It describes the interplay between turbulent motion and mean gas motion, being proportional to the speed of convective elements and to the spatial derivative of the scaled mean velocity field, U/R. It always damps the pulsations and contributes to the driving of turbulent energy[1].

The crucial difference between our and the Florida-Budapest formulation is the treatment of the turbulent source function in convectively stable ($Y < 0$) regions of the model. In our hydrocode, we allow for negative values of the source function, just as in the original Kuhfuß model ($S \sim Y$). In the Florida-Budapest approach, the source term is restricted to positive values only ($S \sim Y_+$), which is equivalent to the neglect of negative buoyancy. Following the convention introduced in Smolec & Moskalik (2008a), we will denote the convective recipe and models ignoring negative buoyancy as PP models (Florida-Budapest approach), while convective recipe and models including negative buoyancy will be denoted by NN (our default formulation).

Consequences of neglecting negative buoyancy

Using our pulsation hydrocodes, we have performed a detailed comparison of models, differing only in the treatment of the source function (NN vs. PP models). Crucial differences are observed for single-mode limit cycle (full amplitude, monoperiodic oscillation) models. The amplitude of the models neglecting negative buoyancy (PP) is much lower than the amplitude of the models including negative buoyancy effects (NN). The lowering of amplitude in case of the PP models is connected with the eddy-viscous damping of pulsations in the deep convectively stable regions of the model. This damping is clearly visible in the nonlinear work integrals presented in Fig. 1. For the PP model, a significant eddy-viscous damping below zone 70 (marked with arrows in the Figure), not present in the NN model, is visible. These internal zones are convectively stable ($Y < 0$), however, in the PP model significant turbulent energies are present in these zones, and hence eddy-viscous damping is possible. How are these turbulent energies built up? The bottom boundary of the envelope convection zone, connected with hydrogen-helium ionization, is located roughly at zone 70 for both PP and NN models. Below this boundary, turbulent motions are effectively braked in the NN model due to the negative value of turbulent source function (eq. 1). Negative buoyancy slows down the turbulent motions very effectively and eddy-viscous damping is not possible in the inner parts of the model, due to negligible turbulent energies. The situation is different in case of PP models, in which the turbulent source function is set equal to zero in convectively stable layers. Therefore, in these layers, turbulent energies are set by the balance between the turbulent dissipation term (D term in eq. 1), which damps the turbulent motions, and the eddy-viscous term, which drives the turbulent energies. Due to the neglect of negative buoyancy, turbulent motions cannot be braked effectively. On the contrary, they are driven at the cost of pulsation, through the eddy-viscous term. Below the envelope convection zone turbulent energies are as high as $10^9 - 10^{10}$ erg/g – only three orders of magnitude smaller

[1] Exact form of this term differ in different pulsation hydrocodes, see Smolec & Moskalik 2008a, however results presented here are insensitive to these differences.

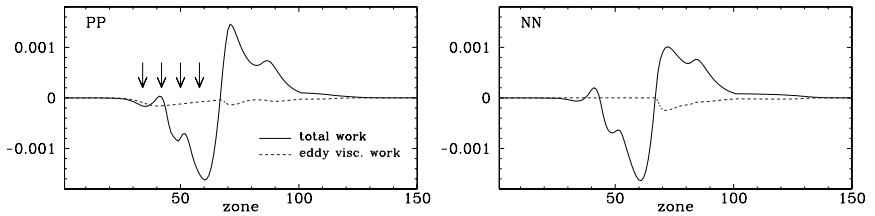

Figure 1: Nonlinear work integrals plotted versus the zone number. Surface at right.

than in the center of the convection zone. Such high turbulent energies extend to more than six local pressure scale heights below the envelope convection zone, leading to significant eddy-viscous damping, visible in the left panel of Fig. 1. Deeper in the envelope, turbulent energies slowly decay, reflecting the vanishing amplitude of the pulsations.

To check the effect of neglecting negative buoyancy on modal selection, we have computed several sequences of nonlinear Cepheid models using both PP and NN convective recipes. Details of mode selection analysis can be found in Smolec & Moskalik (2008b). Each model was initialized (kicked) with several different initial conditions (mixtures of F and 1O linear velocity eigenvectors) and time evolution of the fundamental mode and first overtone amplitudes, A_0 and A_1, was followed. Exemplary results are shown in Fig. 2. The computed trajectories are plotted with solid lines for the PP model and dotted lines for the NN model. Hydrodynamic computations coupled with amplitude equation analysis allow to find all stable pulsation states to which trajectories converge (attractors, solid squares in Fig. 2), and all unstable solutions, that repel the trajectories (open squares in Fig. 2). For single-mode solutions, stability coefficients are computed. These are $\gamma_{1,0}$, which describes the stability of the fundamental mode limit cycle with respect to first overtone perturbation (switching rate toward 1O) and $\gamma_{0,1}$, which measures the stability of the first overtone limit cycle. The negative value of γ means that the respective limit cycle is stable. If both coefficients, $\gamma_{1,0}$ and $\gamma_{0,1}$ are simultaneously positive, both limit cycles are unstable, and double-mode pulsation is unavoidable. The run of stability coefficients across the instability strip, for sequence of Cepheid models, computed with both PP and NN convective recipes, is presented in Fig. 3. The arrow in this Figure marks the location of the model, for which hydrodynamic integrations are presented in Fig. 2.

The amplitude of the given mode is a main factor affecting its stability. The higher the amplitude of the mode, the more able it is to saturate the pulsation instability alone, and hence, the more stable its limit cycle is. For NN models, the amplitude of the fundamental mode is much higher than the amplitude of the first overtone (see Fig. 2) across a significant part of the instability strip. Therefore, the stability coefficient of the fundamental mode limit cycle, $\gamma_{1,0}$, becomes negative, very close to the blue edge of the IS at temperature ≈ 6290K (Fig. 3). A double-mode state is not possible, as first overtone becomes unstable ($\gamma_{0,1} > 0$) for much lower temperature ($T \approx 6165$K). In a temperature range in which both limit cycles are stable, either-or domain is observed, in which pulsation in either limit cycle is possible.

In case of PP models, amplitudes of both modes are reduced as compared to NN models, but not to the same extent. As you can see in Fig. 2, the amplitude of the fundamental mode is much more reduced than the amplitude of the first overtone. This effect is explained by a higher amplitude of the fundamental mode (in comparison to 1O) in convectively stable layers of the PP model, in which significant turbulent energies are observed. As a result, eddy-viscous damping is stronger for the fundamental mode. Differential reduction of mode amplitudes is crucial in bringing up double-mode behaviour in the PP model sequence. At the hot side of the IS, the amplitude of the fundamental mode is lower, or comparable to the amplitude of the first overtone. Hence, the fundamental mode limit cycle is unstable

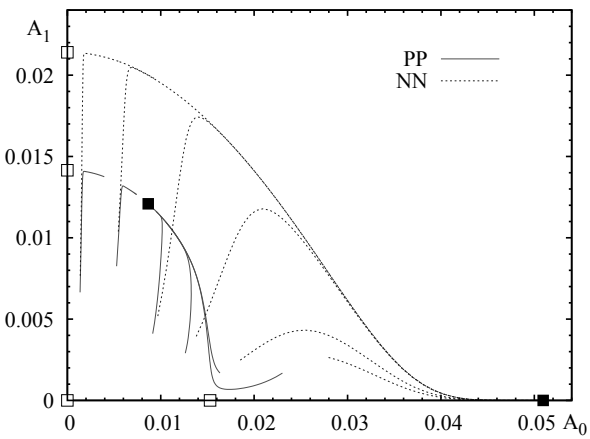

Figure 2: Hydrodynamic integrations for a particular Cepheid model. Solid lines - model computed with PP convection, dotted lines model computed with NN convection.

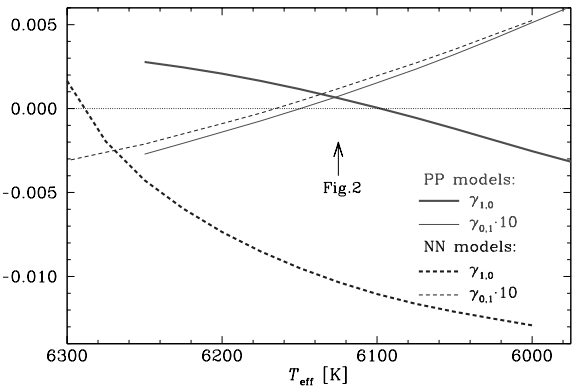

Figure 3: The run of stability coefficients along a sequence of Cepheid models of constant mass/luminosity. Solid lines for the PP models, dashed lines for the NN models.

($\gamma_{1,0} > 0$) in a wide temperature range. It becomes stable at much lower temperature ($T \approx 6100$K) in comparison to the NN sequence. At this temperature, the first overtone is already unstable. Consequently, in a relatively wide temperature range ($\sim$ 50K in Fig. 3), both limit cycles are unstable and double-mode state emerges.

Summary

Neglect of negative buoyancy has serious consequences for the computed Cepheid models. It leads to high turbulent energies in convectively stable layers, and consequently to strong eddy-viscous damping. This damping acts differentially on pulsation modes, which promotes the

double-mode behaviour. If buoyant forces are taken into account, as they should be, no stable nonresonant double-mode behaviour can be found (Smolec & Moskalik 2008b). Therefore, the problem of modeling F/1O double-mode behaviour in classical Cepheids remains open.

Acknowledgments. I am very grateful for many fruitful discussions with Pawel Moskalik and Wojciech Dziembowski. Pawel Moskalik is acknowledged for reading the manuscript. I am grateful to the referee, Geza Kovács, for many comments on the presented results. The author is grateful to the EC for the establishment of the European Helio- and Asteroseismology Network HELAS, as well as for the financial support, which made the participation of the author to this workshop possible. This work has been supported by the Polish MNiSW Grant No. 1 P03D 011 30.

References

Feuchtinger, M. 1998, A&A, 337, 29

Kolláth, Z., Beaulieu, J. P., Buchler, J. R., et al. 1998, ApJ, 502, L55

Kolláth, Z., Buchler, J. R., Szabó, R., et al. 2002, A&A, 385, 932

Kovács, G., & Buchler, J. R. 1993, ApJ, 404, 765

Kuhfuß, R. 1986, A&A, 160, 116

Smolec, R., & Moskalik, P. 2008a, AcA, 58, 193

Smolec, R., & Moskalik, P. 2008b, AcA, 58, 233

DISCUSSION

Kovács: Let me note that purely radiative RR Lyrae models with a proper choice of the artificial viscosity lead also to sustained double-mode models (see Kovács & Buchler 1993). Furthermore, the convective models of Buchler and coworkers (e.g. Kolláth, Buchler, Szabó et al. 2002) have been able to reproduce the bulk properties of the observed double-mode RR Lyrae and δ Cephei stars. The former ones were successfully modeled also by Feuchtinger (1998), who used similar type of convective modeling as Kolláth, Buchler & Szabó.

Smolec: Radiative double-mode models of Kovács & Buchler were obtained by decreasing artificial viscosity. These models are sensitive to numerical details and do not reproduce all observational constraints. Detailed comparison of nonlinear convective double-mode models of Buchler and coworkers with observations (Fourier decomposition of light curves) was not performed. Using Vienna pulsation hydrocode Feuchtinger (1998) computed one double-mode RR Lyrae model. This is the only double-mode model published by the Vienna group. As both Florida-Budapest and Vienna codes are claimed to give essentially the same results in case of single-mode models (Feuchtinger, Buchler & Kolláth 2000), we suspect that also in the Vienna code negative buoyancy was neglected. However, as we haven't computed any RR Lyrae models, we cannot make definite statements about double-mode RR Lyrae models.

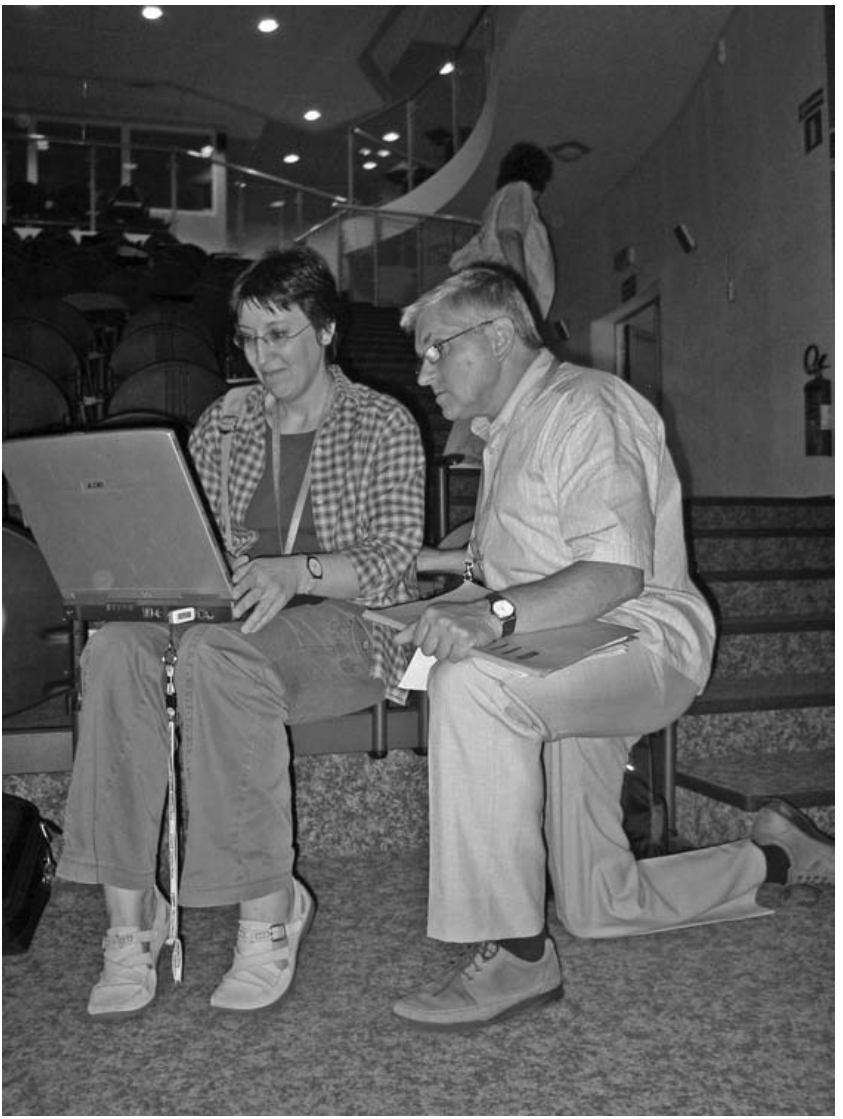

Josefina Montalbán and Alosha Pamyatnykh have something interesting to discuss.